NUCLEAR STRUCTURE -- EXPERIMENTAL

^{12}C OPTICAL POTENTIALS AT E/A = 70 MeV.

J.S. Winfield, A. Nadasen[a], N. Anantaraman, S.M. Austin, J.A. Carr[b], C. Djalali, A. Gillibert[c], W. Mittig[c], J.A. Nolen and Z. Wenlong[c]

In the course of a charge exchange measurement at GANIL (see contribution elsewhere in this report), elastic and inelastic scattering data were taken on ^{26}Mg and ^{54}Fe targets with an E/A = 70 MeV ^{12}C beam. These data were measured over a limited angular range (2.0° to 4.75° in the laboratory), and were primarily intended to evaluate the optical potentials used in the charge exchange DWBA calculations, since no potentials could be found in the literature for the same energy and target-projectile combinations we used. (We also measured ^{12}C+^{90}Zr scattering, but the data were too limited in angular range to show any significant sensitivity to the nuclear potential.) Measurements at high incident energy are interesting because it has been possible to find unique potentials,[1] in contrast to energies below about E/A = 20 MeV where ambiguities in the multi-parameter space are prevalent.

The data are shown in Figs. 1 and 2. We note that the cross sections for inelastic scattering to the collective 2^+ states are large and are already comparable with those for elastic scattering at 3.5° c.m. for ^{26}Mg and at 5.5° c.m. for ^{54}Fe

Since the optical potentials were to be used in DWBA charge exchange calculations, it was important to use the DWBA formalism for the elastic and inelastic scattering calculations. Accordingly, PTOLEMY (Ref. 2) was used rather than a coupled-channels program. The macroscopic model was assumed for the inelastic excitation, in which the derivative of the scattering potential is used as the effective interaction.

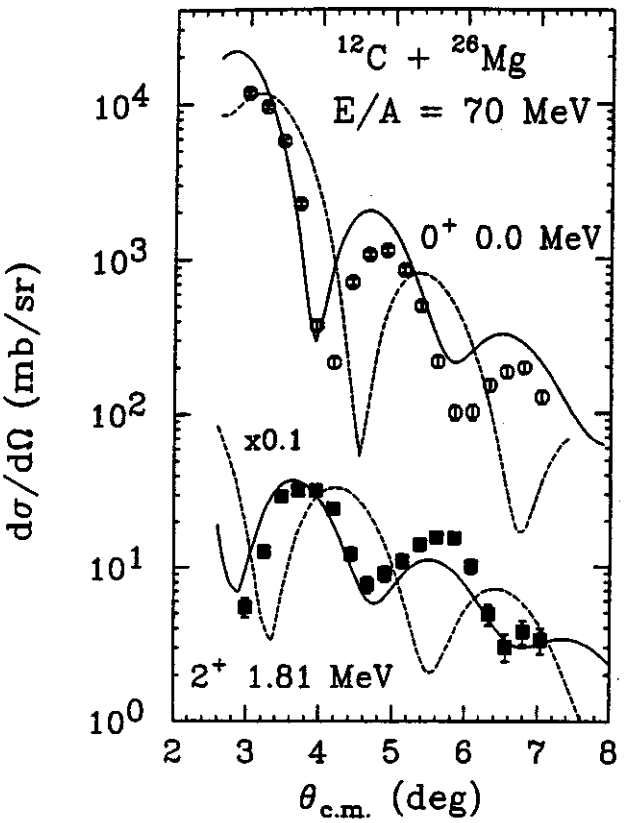

Fig. 1 Elastic and inelastic scattering of ^{12}C on ^{26}Mg at E/A = 70 MeV. The curves are DWBA calculations with the following optical potentials: ^{16}O+^{28}Si from Ref. 4 (solid lines), ^{12}C+^{12}C from Ref. 3 (dashed lines). The inelastic scattering cross sections have been scaled by 0.1 for display purposes.

Figure 1 shows that the E/A = 84 MeV ^{12}C+^{12}C potential from Buenerd et al.[3] is badly out of phase with our ^{12}C+^{26}Mg elastic and inelastic scattering data. The E/A = 94 MeV ^{16}O+^{28}Si potential from Roussel et al.[4] gives better agreement, but still overpredicts the elastic scattering data beyond 4°. (All potentials are listed in Table I.)

Figure 2 shows the differential cross section for ^{12}C+^{54}Fe elastic and inelastic scattering. The ^{16}O+^{40}Ca potential taken from

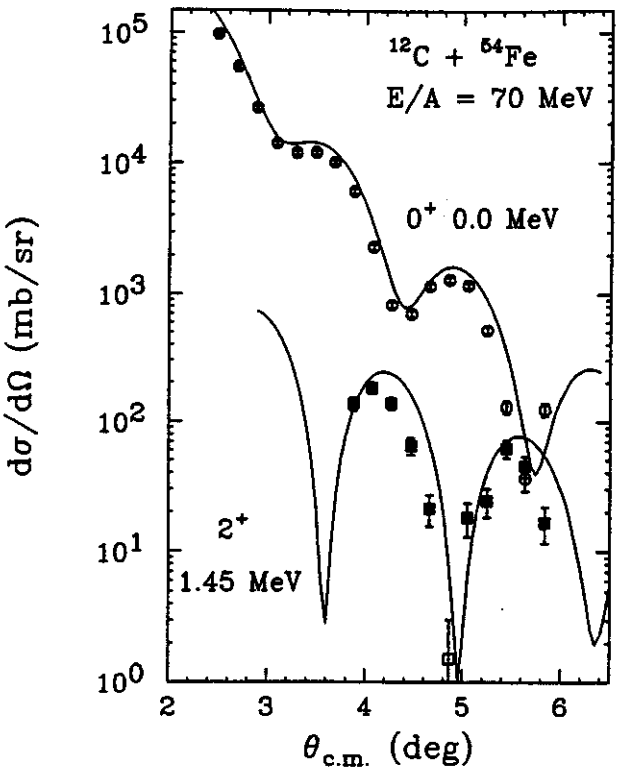

Fig. 2 Elastic and inelastic scattering of ^{12}C on ^{54}Fe at E/A = 70 MeV. The curves are DWBA calculations with the $^{16}O+^{40}Ca$ optical potential from Ref. 4.

Table I. Woods-Saxon optical model potentials. "System" and "E/A" refer to the scattering system and bombarding energy for which the potential was derived. The convention $R = r(A_T^{1/3}+A_P^{1/3})$ is used. Potential strengths are in MeV, radii and diffusenesses are in fm, and volume integrals are in MeV·fm^3.

System	E/A	V	r_v	a_v	W	r_w	a_w	J_v/A	J_w/A	Ref.
$^{12}C+^{12}C$	85	120	0.71	0.84	34.0	0.96	0.69	125	69	3
$^{16}O+^{28}Si$	94	100	0.892	0.905	50.5	0.992	0.780	151	95	4
$^{12}C+^{26}Mg$	70	82	0.863	0.901	38.0	0.917	1.110	143	87	(a)
$^{12}C+^{26}Mg$	70	-	-	-	38.0	0.921	1.265	236	97	(b)
$^{16}O+^{40}Ca$	94	60	1.042	0.710	54.1	1.042	0.710	105	95	4

a) Fitted Woods-Saxon potential.

b) Woods-Saxon imaginary potential used in conjunction with real folded potential.

Ref. 4 gives a reasonable description of the elastic scattering data, given the ±12% experimental uncertainty in the absolute cross section. However, the inelastic scattering prediction is slightly out of phase with the data -- perhaps indicating a deficiency in this potential not revealed by the limited elastic scattering data.

The deformation parameters and lengths deduced from the inelastic DWBA analysis are listed in Table II, and compared with values from other work. The Roussel et al. potentials give reasonable agreement for both targets. The values from the Buenerd et al. potential are worse, as expected from the disagreement with the shape of the angular distribution.

In view of the poor fits to the $^{12}C+^{26}Mg$ elastic scattering data, we attempted to find our own potentials. Since the present data alone are far too limited to provide unambiguous potentials, we adopted the following approaches. First, the expected volume integrals of Woods-Saxon potentials were predicted by interpolating the energy and mass trends observed in Refs. 5 and 6. The predicted volume integrals for E/A = 70 MeV $^{12}C+^{26}Mg$ are 145 and 74 MeV·fm^3 for the real and imaginary potentials, respectively. The second approach was to use a microscopic real potential, obtained from double-folding the nucleon-nucleon interaction with the target and projectile densities. This was done with the program FOLD.[7] Neither of the above approaches are sufficient to define the complete optical potential: the radii and diffusenesses of the Woods-Saxon potentials have to be obtained from fits to the elastic scattering data, and a phenomenological imaginary potential is needed to supplement the real folded potential. In the fitting procedure, the depths of the interpolated potential were not adjusted to help keep the volume integrals constant -- this is a possible future improvement. For the folded potential case, a Woods-Saxon imaginary

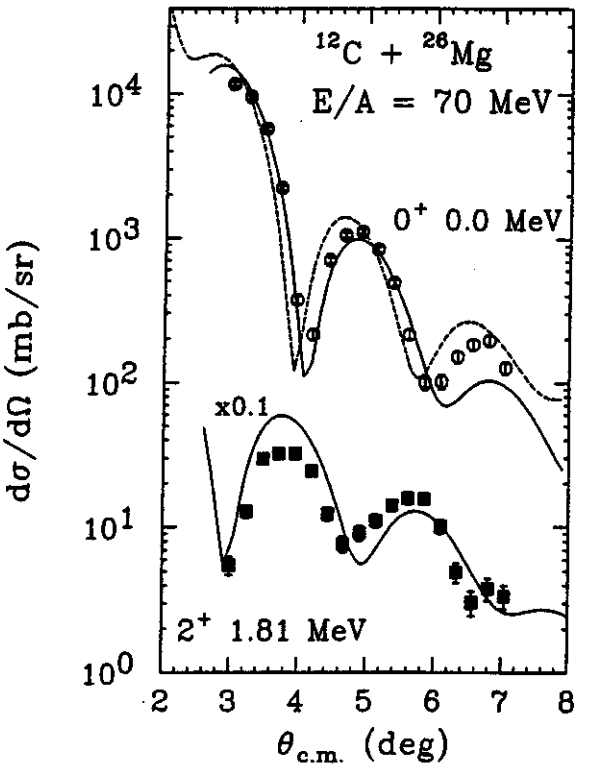

Fig. 3 Same as Fig. 1 except that the curves are the results of the fitted Woods-Saxon (solid lines) and real folding model (dashed line) potentials.

potential was independently fitted to the data. The parameters of the fitted Woods-Saxon potentials are listed in Table I.

The fits to the elastic scattering data and the inelastic scattering predictions (in the case of the Woods-Saxon potential) are shown in Fig. 3. The shape of the inelastic angular distribution predicted by the Woods-Saxon potential agrees quite well with the data, but the values of β_2 and δ_2 are unacceptably high (Table II). This may be associated with the fitted Woods-Saxon potential having an imaginary volume integral (87 MeV.fm^3) significantly larger than the predicted value.

In conclusion, it is apparent that inelastic scattering data are useful to test optical potentials, especially when the elastic scattering data are limited in angular extent. Presumably this is because different reactions

Table II. Deformation parameters and lengths derived from inelastic scattering analyses. The deformation length is defined as $\delta = R'\beta$, where $R' = r_v A_T^{1/3}$ (see Ref. 2). For comparison, values from the literature for other projectiles are given.

Excited state	Reaction	β_2	δ_2 (fm)	Note
^{26}Mg 1.81 MeV	(^{12}C,^{12}C')	0.45	0.95	^{12}C+^{12}C potl. (Ref. 3)
		0.32	0.85	^{16}O+^{28}Si potl. (Ref. 4)
		0.52	1.33	fitted ^{12}C+^{26}Mg potl.
	(^{9}Be,^{9}Be')	0.30	0.84	Ref. 8.
	(α,α')	0.29	0.74	Ref. 9.
^{54}Fe 1.45 MeV	(^{12}C,^{12}C')	0.18	0.71	^{16}O+^{40}Ca potl. (Ref. 4)
	(p,p')	0.16	0.76	Ref. 10.

are sensitive to somewhat different radial regions of the effective interaction. Volume integrals may be an additional guide for light heavy-ions, but they are clearly not sufficient if the data set is limited. Further investigation needs to be done with folded potentials; for instance, one might try an imaginary potential which has the same shape as the real potential.

a. University of Michigan, Dearborn, MI.
b. Florida State Univ., Tallahassee, FL.
c. GANIL, Caen, France.

References

1. G.R. Satchler, Nucl. Phys. A505, 103 (1989); A. Nadasen et al., Phys. Rev. C40(1989)1237.
2. M.H. Macfarlane and S.C. Pieper, Argonne National Laboratory Report No. ANL-76-11, 1976.
3. M. Buenerd et al., Nucl. Phys. A424(1984)313.
4. P. Roussel et al., Nucl. Phys. A477(1988)345.
5. A. Nadasen et al., Phys. Rev. C39(1989)536.
6. M.E. Brandan, Phys. Rev. Lett. 60(1988)784.
7. J. Cook and J.A. Carr, Florida State Univ., 1988 (unpublished); based on the formalism of F. Petrovich et al., Nucl. Phys. A425(1984)609.
8. J.S. Winfield, D.Phil. thesis, Oxford (1983).
9. I.M. Naqib and J.S. Blair (unpublished); quoted in H. Rebel et al., Nucl. Phys. A182(1972)145.
10. S.F. Eccles, H.F. Lutz and V.A. Madsen, Phys. Rev. 141(1966)1067.

HIGH LYING STATES OBSERVED IN HEAVY ION TRANSFER REACTIONS

G.M. Crawley, G. Yoo, S.M. Austin, C. Djalali[a], W. Benenson, J. Winfield,
S. Fortier[b] and S. Gales[b]

During the past few years, information about deep hole states and high lying single particle states in several medium and heavy nuclei has been obtained by studying light ion reactions such as (p,d), (^{3}He,α) and (α,^{3}He).[1] Due to the selectivity of these reactions for transferring large values of angular momentum, the excitation of nucleons into high spin orbitals was observed as large resonance-like bumps located at high excitation energy. It appears useful to investigate the possible use of heavy ion reactions at high incident energies. In some cases these reactions are even more selective in exciting high spin states, the peak-to-background ratios may be more favorable and also the excitation cross section are larger than in the corresponding light ion one-nucleon transfer reactions.

This work reports an investigation of one-nucleon-transfer reactions induced by ^{20}Ne ions on ^{90}Zr and ^{208}Pb.. The experiment was performed at incident energies of 500 and 600 MeV in order to disentangle transfer from three-body processes. Calculations using the exact finite range distorted wave Born approximation (EFR-DWBA) method were also performed and these results are compared with the data. The main features of the spectra observed in pick-up reactions and particularly the low excitation energy part of the stripping spectra are qualitatively well reproduced by DWBA calculations which include mutual excitation of the target and ejectile nuclei. At an excitation energy close to that of the Giant Quadrupole Resonance in the corresponding target nucleus, the ^{90}Zr(^{20}Ne,^{19}Ne) and ^{208}Pb(^{20}Ne,^{19}Ne) spectra are dominated by a few MeV wide structure superimposed on a large bump due to fragmentation processes. It is proposed that this structure arises from neutron transfer to high spin orbitals.

The measurements were carried out using 500 and 600 MeV ^{20}Ne beams from the K500 superconducting cyclotron at Michigan State University. The isotopic enrichments of the 1.0 mg/cm^2 thick ^{90}Zr and 3.0 mg/cm^2 thick ^{208}Pb targets were 98.5% and 99.9% respectively. The reaction products were analyzed with the S320 broad range magnetic spectrograph and detected by the standard focal plane detector system (two resistive wire position counters, two ionization chambers and a plastic scintillator), ensuring unambiguous particle discrimination. A thin film start detector was used together with the plastic scintillator to obtain the time of flight of ions through the spectrograph. The calibration of the focal plane was determined independently for each incident energy and each target nucleus by measuring the position of the elastic peak along the counter for different magnetic fields. The overall energy resolution $\Delta E/E$ measured for the elastic peak varied from about 2.10^{-3} to 4.10^{-3} depending on its position along the focal plane. Spectra obtained at the grazing angle for both target nuclei at both incident energies are displayed in Figs. 1-2. The accuracy of the value of this summed excitation energy (also labelled Q_{gg}-Q in the spectra) is estimated to be better than 1 MeV.

Apart from the contribution of three-body reactions, the spectra of Figs. 1-2 are expected to result from the addition of the various experimentally unresolved mutual excitations of the final nuclei. The shapes observed for these spectra suggest that some combinations of configurations are favoured in the present transfer reactions. In order to test this interpretation, DWBA calculations were performed

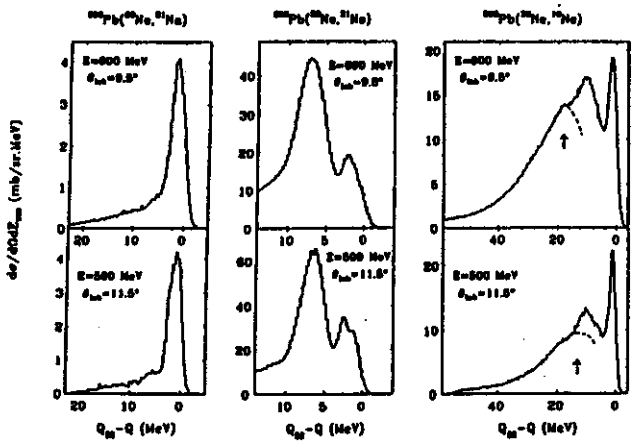

Fig. 1. Experimental spectra from the ^{20}Ne + Pb ^{208}reactions at 500 and 600 MeV. The arrow indicates the position of the ^{19}Ne ions moving with the beam velocity. The shape of the low-excitation-energy side of the break-up bump is suggested by dashed lines.

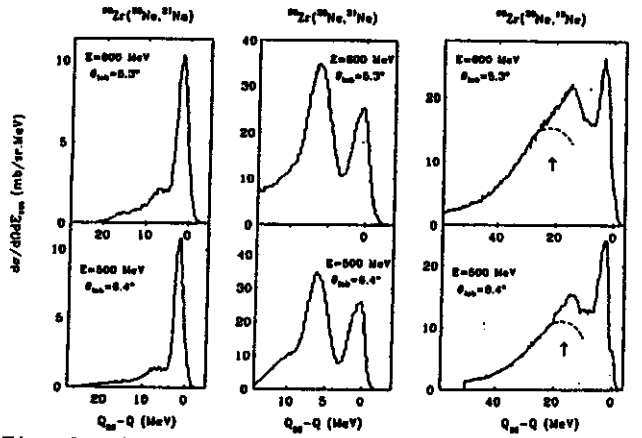

Fig. 2. Experimental spectra from the ^{20}Ne + Zr ^{90}reactions at 500 and 600 MeV. The arrow indicates the position of the ^{19}Ne ions moving with the beam velocity. The shape of the low-excitation-energy side of the break-up bump is suggested by dashed lines.

at 500 and 600 MeV. Recent high resolution studies of one-nucleon transfer reactions induced by ^{12}C and ^{16}O of a few hundred MeV[2-4] show that the relative cross sections for excitation of different configurations could be well reproduced by DWBA calculations.

The DWBA calculations were performed with full recoil finite range program Ptolemy.[5] In the absence of elastic scattering data for all systems under study, the same optical model potential[6] was used for the interaction of ^{20}Ne with ^{90}Zr and ^{208}Pb at both incident energies.

The following procedure was adopted in order to compare the results of DWBA calculations to the data since individual levels in the light and heavy final nuclei could not be resolved experimentally. Theoretical spectra for each reaction at a particular angle and incident energy were first deduced from the DWBA cross sections weighted by the spectroscopic factors of the main single-particle and single-hole states in the final nuclei. These theoretical spectra were then convoluted with a gaussian shape (simulating the experimental energy resolution) and multiplied by a normalization factor in order to compare with the experimental results. The full width at half-height of the gaussian and the normalization factor were both adjusted in order to fit the low excitation energy part of the experimental spectra, where uncertainties about the distribution of spectroscopic strengths are smaller.

An example of the experimental and the convoluted theoretical ^{21}Na spectra at 500 MeV incident energy are displayed in Fig. 3. The positions and predicted strengths of the peaks are marked as vertical lines in the figures.

The experimental shapes of the bumps in the ^{21}Na + ^{89}Y and ^{21}Na + ^{207}Tl spectra are qualitatively well reproduced by DWBA calculations by assuming an experimental resolution of 1.6 MeV, as shown in Fig. 3. The ^{89}Y spectrum is consistent with a preferential excitation of the 2p3/2 state at 1.51 MeV in ^{89}Y, whereas the 3s1/2, 2d3/2, 1h11/2 and 2d5/2 single-proton-hole states below 1.7 MeV in ^{207}Tl are predicted to contribute almost equally to the cross section.

Various three-body reactions are also expected to contribute to the high-lying part of the ^{19}Ne spectra. Structures originating from a three-body contribution should be observed at apparent excitation energies which move with incident energy according to the kinematics of the reaction. The position of the bumps observed at 10 MeV and 14 MeV summed excitation energy in the ^{208}Pb(^{20}Ne,^{19}Ne)^{209}Pb and

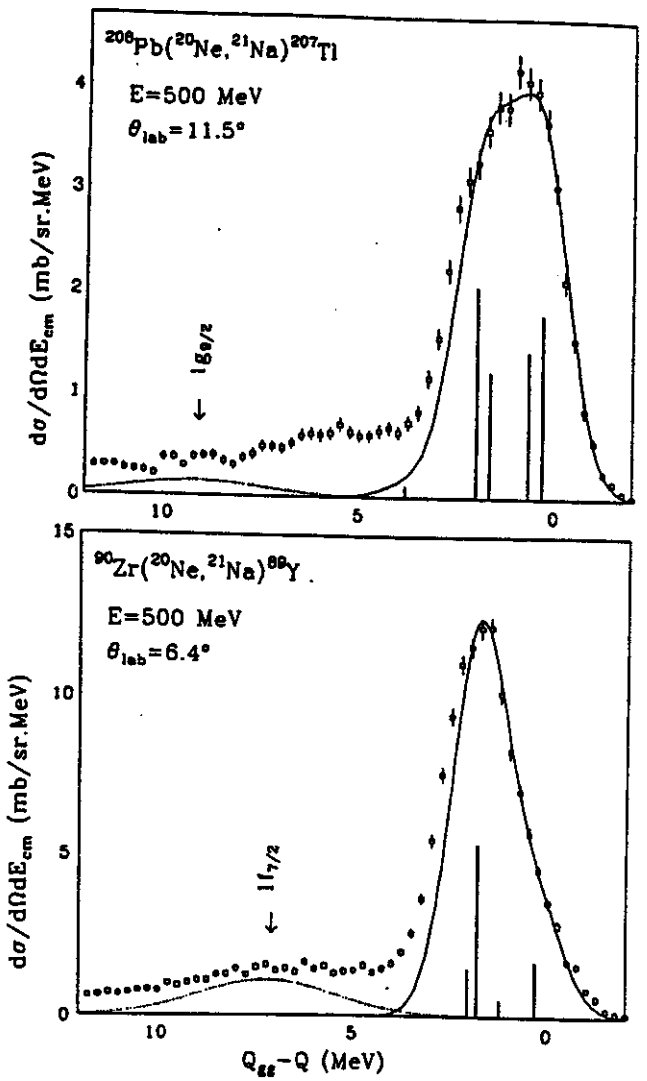

Fig. 3. Comparison between experimental ^{21}Na spectra (points with error bars) and calculated ones (full line) using a resolution parameter of 1.5 MeV. (The normalization factors were 1.80 and 1.19 for ^{89}Y and ^{207}Tl, respectively.) The DWBA predicted contributions of various combinations of configurations in ejectile and residual nuclei are represented by the length of vertical bars. The dotted line at high excitation energy represents the calculated contribution of transfer to the internal 1f7/2 and 1g9/2 subshells in ^{89}Y and ^{207}Tl, respectively.

$^{90}Zr(^{20}Ne,^{19}Ne)^{91}Zr$ reactions respectively, is independent of incident energy. This suggests that these structures result from a neutron transfer to an unbound state in the residual heavy nucleus.

We conclude that the low excitation energy parts of the present one-nucleon transfer spectra are qualitatively well reproduced by DWBA calculations. Ejectile excitations are clearly responsible for the major differences in the spectra observed in the proton and neutron pick-up reactions: the high excitation energy bump in the ($^{20}Ne,^{21}Ne$) reaction is related to the mutual excitation of 1d3/2, 1p3/2, 1f7/2 shell model states in ^{21}Ne and neutron-hole states in the heavy nucleus, whereas the excitation of mirror states in ^{21}Na does not contribute to the proton pick-up spectra since these states are unbound. The ($^{20}Ne,^{19}Ne$) transfer reaction is dominated by transfer to high spin single particle states in the heavy residual nucleus. Structures observed at high excitation energy in the ^{19}Ne spectra are interpreted as unbound single particle states resulting from a neutron transfer in a high spin external orbital. Any further investigation to confirm the present conclusions and eventually to investigate other higher lying single particle states requires a more precise determination of the underlying three-body continuum or a strong reduction of this background through coincidence experiments.

We acknowledge fruitful discussions with J. Barrette and D. Brink.

---

a. University of South Carolina
b. IPN, Orsay

References

1. S. Gales, Ch. Stoyanov and A.I. Vdovin, Phys. Reports 166(1988)127. and refs. therein.
2. M.C. Mermaz et al., Z. Phys. A326(1987)353.
3. E. Tomasi-Gustaffson, These Universite Paris-Sud (1988). M.C. Mermaz et al, Phys. Rev. C37(1988)1942 et refs. therein.
4. J.S. Winfield, E. Adamides, S.M. Austin, G.M. Crawley, M.F. Mohar, C.A. Ogilvie, B. Sherrill, M. Torres, G. Yoo and A. Nadasen, Phys. Rev. C39(1989)1395.
5. M.H. Macfarlane and S.C. Pieper, Argonne National Laboratory, Report ANL-76-11 (1976).
6. M. Buenerd, J. Chauvin, G. Duhamel, J.Y. Hostachy, D. Lebrun, P. Martin, P.O. Pellegrin, G. Perrin and P. de Saintignon, Phys. Lett. 167B(1986)379.

GAMOW-TELLER β^+ STRENGTHS IN Fe NUCLEI FROM THE (^{12}C,^{12}N) REACTION AT E/A = 70 MeV

N. Anantaraman, J.S. Winfield, Sam M. Austin, C. Djalali, J.A. Nolen, Jr., A. Gillibert[a], Zhan Wenlong[a], W. Mittig[a] and J.A. Carr[b]

As reported in the 1987 Annual Report, the (^{12}C,^{12}N) reaction was measured on targets of $^{54,56,58}Fe$ at an energy of 70 MeV/nucleon at Laboratoire GANIL in late 1987 by a MSU/GANIL collaboration. The goal was to obtain Gamow-Teller (GT) strengths in the β^+ direction for low-lying levels in the Mn nuclei. The strategy adopted was to use the (^{12}C,^{12}B) reaction, leading to states of known B(GT), to provide a calibration curve. For this purpose, the (^{12}C,^{12}B) reaction was studied on targets of ^{12}C, ^{26}Mg, ^{54}Fe, ^{58}Ni and ^{90}Zr.

An analysis of the data in terms of distorted-wave Born approximation (DWBA) predictions shows several characteristic features. These features are illustrated in Fig. 1, which shows an angular distribution for $^{26}Mg(^{12}C,^{12}B)^{26}Al$. All angular distributions for $0^+ \rightarrow 1^+$ transitions exhibit appreciable L=2 components, even at 0°. This L=2 strength is much larger than seen in (p,n) reactions at small angles and presumably arises from the large negative Q values associated with the reactions and the accompanying large value of the momentum transfer q. The L=2 strength is dominantly from the tensor force whose strength grows rapidly with increasing momentum transfer. Since the tensor force does not mediate β-decay transitions, we have chosen to subtract the L=2 strength before using these cross sections to obtain GT strengths.

In order to establish the utility of the (^{12}C,^{12}B) and (^{12}C,^{12}N) reactions as spin probes, we have performed a number of tests, some experimental and some in the nature of computer experiments. DWBA calculations showed (1) that most of the complicated amplitudes, involving L = 0, 2 contributions from both the projectile and target, were small and did not

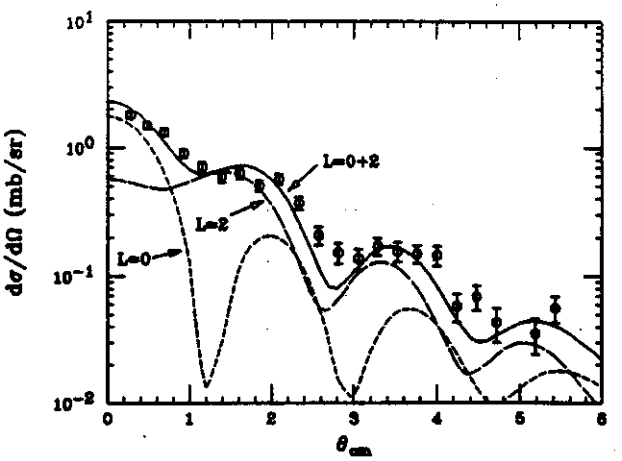

Fig. 1. Angular distribution for the $^{26}Mg(^{12}C,^{12}B)^{26}Al(1^+, 1.06\ MeV)$ reaction at 70 MeV/nucleon. The short dash curve is for L=0, the long dash curve for L=2 and the solid curve, the sum of the L=0 and L=2 contributions.

disturb conclusions based on simple calculations; (2) that different effective interactions yielded cross sections having mainly normalization differences which cancel in the calibration procedure developed later; and (3) that cross sections of L=0 transitions are closely proportional to B(GT) values calculated with the same wave functions. This latter point is a fundamental requirement if these reactions are to serve for spin spectroscopy. The point is found to be satisfied even though heavy-ion reactions in general sample only the surface parts of the GT transition densities. The example of $^{26}Mg(^{12}C,^{12}B)^{26}Al$ is shown in Fig. 2; the proportionality requirement is fairly well satisfied even for weak GT transitions such as those to states 4 and 5.

The DWBA calculations used the code FOLD based upon the momentum space techniques developed by Petrovich and his co-workers.[1] The 100 MeV t-matrix interaction of Franey and Love[2] was used and exchange was included for the

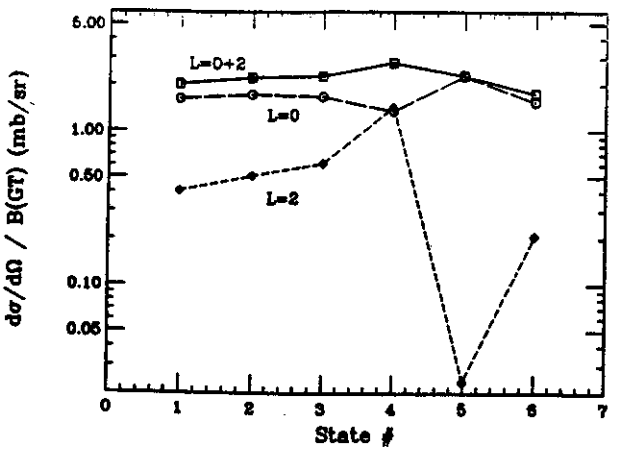

Fig. 2. Ratios of DWBA zero degree cross sections and B(GT) values calculated with full-sd-shell wave functions for the six lowest lying 1^+ states in ^{26}Al.

central interaction. Effects of the tensor exchange are expected to be small.[3] For the ^{26}Mg→^{26}Al transitions, we used the full sd shell wave functions of Brown and Wildenthal[4]; for other nuclides, less complete wave functions were available. It was found that the calculated L=0 and L=2 strengths depended somewhat on the details of the wave functions, but that the shapes did not. The optical model potentials used were those obtained for ^{16}O scattering at 94 MeV/nucleon by Roussel-Chomaz et al.[5] except for ^{12}C where the potential set F of Buenerd et al.[6] was used. It is difficult to evaluate the uncertainties introduced by lack of optimum optical model potentials, but differences of perhaps 30% seem possible. Cohen-Kurath wave functions were used to describe the projectile and ejectile; a correction was made to account for the fact that these wave functions do not exactly reproduce the B(GT) for ^{12}B and ^{12}N.

The resulting cross sections were generally in good agreement with the measured cross sections, requiring normalizations of 30% or less, an amount certainly in the range of the overall calculational uncertainties. In many cases the angular distributions were well described quantitatively. In other cases the agreement was only qualitative. However, it was generally possible to obtain good agreement by adjusting the relative strengths of the L=0 and L=2 contributions, i.e. by performing a multipole decomposition.

Given the situation above, the following procedure was used to check the consistency of the extracted unit cross sections, the ratio of the cross section measured at q=0 to the GT strength B(GT). First, calculations were made as outlined above, to provide L=0 and L=2 angular distributions. The relative strengths of these distributions were adjusted to yield the best least squares fit to the cross section. Fortunately, the L=0 and L=2 amplitudes have very distinctive shapes, making this separation unambiguous for sufficiently accurate data. This yielded the L=0 cross section at 0°, i.e. at zero transverse momentum transfer. In order to obtain the cross section corresponding to a total momentum transfer q=0, this cross section was multiplied by the ratio R of the L=0 cross section calculated at Q=0 MeV to that at the actual Q of the reaction (typically around -20 to -30 MeV). Dividing this cross section by the corresponding B(GT) leads to the calibration line shown in Fig. 3. For want of a better theoretical form for the A-dependence of the curve, a linear form was assumed for it and its parameters were determined by least-squares fitting. This line can be used to obtain the B(GT) from the cross section measured for an unknown transition.

Preliminary attempts have been made to use this calibration line and the results obtained for ^{56}Fe(^{12}C,^{12}N)^{56}Mn to extract B(GT) for transitions to the two lowest lying 1^+ states in ^{56}Mn, to provide a check on the electron capture strengths used in supernova calculations. The calculations appear to agree better with the results of Brown[7] than with those of Bloom and Fuller.[8] However, the data for (^{12}C,^{12}N) generally have less statistics than the (^{12}C,^{12}B) results and, for the ^{56}Fe case, the L=2 strengths are rather large, so that the results are not conclusive. Measurements at

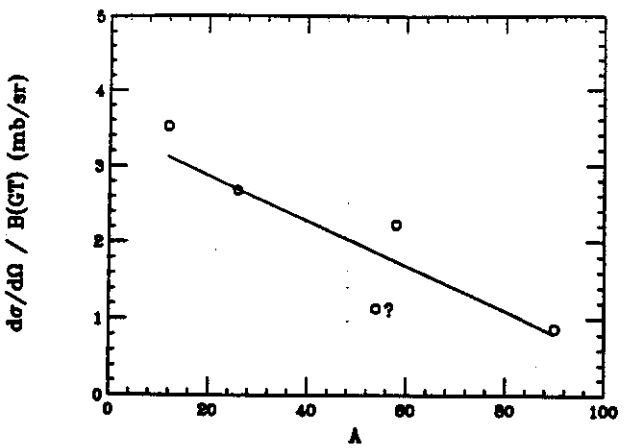

Fig. 3. Calibration line determined from the (^{12}C,^{12}B) reaction on several nuclei as described in the text. The data for ^{54}Fe are less complete than those for the other targets.

higher energies may help to resolve this problem.[9]

---

a. Laboratoire GANIL, Caen, France.
b. Florida State Univ., Tallahassee, Florida.

References

1. J. Cook and J.A. Carr, computer program FOLD, Florida State University 1988 (unpublished); based on the formalism of F. Petrovich et al., Nucl. Phys. A425(1984)609.
2. M.A. Franey and W.G. Love, Phys. Rev. C 31(1985)488.
3. A. Etchegoyen, E.D. Izquierdo and M.C. Etchegoyen, Phys. Lett. 231B(1989)224.
4. B.H. Wildenthal, Prog. Part. Nucl. Phys. 11(1984)5; B.A. Brown and B.H. Wildenthal, Ann. Rev. Nucl. Part. Sci. 38,29(1988).
5. P. Roussel-Chomaz, N. Alamanos, F. Auger, J. Barrette, B. Berthier, B. Fernandez and L. Papineau, Nucl. Phys. A477(1988)345.
6. M. Buenerd, A. Lounis, J. Chauvin, D. Lebrun, P. Martin, G. Duhamel, J.C. Gondrand and P. de Saintignon, Nucl. Phys. A424(1984)313.
7. B.A. Brown, private communication.
8. S. Bloom and G. Fuller, Nucl. Phys. A440(1985)522.
9. H. Lenske, H.H. Wolter and H.G. Bohlen, Phys. Rev. Lett. 62(1989)1457.

IN-BEAM γ-RAY SPECTROSCOPY OF ODD-ODD ^{176}Re: DOUBLY-DECOUPLED AND COMPRESSED BANDS

W.-T. Chou, W.A. Olivier, A. Rios, Wm.C. McHarris and R. Aryaeinejad[a]

Studies of deformed odd-odd nuclei have become more intense during the past few years, including a number of nuclei in the Ta-Re-Ir region.[1-4] The in-beam γ-ray spectra of these nuclei are simpler than might be expected at first, most likely because heavy-ion-induced reactions tend to populate states highly aligned with rotation, and the subsequent γ deexcitation favors similar (coriolis-connected) states.[1-5] The advantages of this are that only a selected subset of lower-lying bands is populated strongly, making the analysis much more tractable; the drawback, what we can learn from heavy-ion-induced reactions is limited more or less to these few bands. More often than not, the ground-state band is not strongly populated, and the strongly-populated bands feed into the lowest states via low-energy, highly-converted, and/or delayed transitions, the result being that very few such connections have been worked out. Thus, assigning spins and structures to the observed bands requires relying more than usual on understanding the neighboring odd-mass nuclei and on systematics.

Santos et al.[4] used the ^{169}Tm(^{12}C,5nγ) reaction for the first studies of ^{176}Re. Their level scheme included parts of two rotational bands. One of these is the so-called doubly-decoupled band, a type of band first observed in the Ta-Re-Ir region by Kreiner et al.[2] They interpreted it as a coupling of the $\pi 1/2^-[541]$ and $\nu 1/2^-[521]$ states, both of which drop to rather low excitation energies in the more neutron-deficient Re nuclei. The second band could be interpreted as a coupling of $\pi 5/2^+[402]$ and $\nu i_{13/2}$ states. A similar band had been found[5] in ^{180}Re, its main characteristic being that the moment of inertia changes rapidly with consecutive band members, especially toward the bottom of the band. Such behavior is typical of bands involving $i_{13/2}$ neutron states with strong coriolis coupling.

Here, we present initial results from our in-beam γ-ray spectroscopic studies, in which we used heavier projectiles and were able to extend the reported bands to much higher spin. These studies allow us to extract the backbending frequency for the doubly-decoupled band, and we compare this with backbending behavior in the neighboring even-even and odd-mass nuclei. We disagree somewhat with Santos et al. as to the structure of the second band. Since interacting-boson-fermion-fermion-approximation calculations[7,8] (IBFFA, IBA calculations extended to odd-odd systems) have proven their ability to predict excitation-energy spectra satisfactorily, we make new use of our calculations to assist in interpreting this band.

We produced ^{176}Re by the ^{159}Tb(^{22}Ne,5nγ) reaction, using a 113-MeV ^{22}Ne beam from the MSU NSCL K500 cyclotron. Two primary Ge detectors were used, each having a NaI(Tl) annulus as a compton shield, placed at ±90° with respect to the beam direction. A low-energy photon spectrometer (LEPS) was placed at 125° to help resolve and distinguish low-energy γ-rays. In addition, a time-to-amplitude converter (TAC) was used to study time relationships among the γ transitions and to measure the half-lives of any observed metastable states. For experimental details and examples of spectra, see Ref. 9.

A second set of experiments was performed using the ^{165}Ho(^{16}O,5nγ) reaction, with a 97-MeV ^{16}O beam provided by the SUNY Stony Brook tandem-linac. For these experiments we used the standard SUNY-SB six-detector BGO-shielded Ge-detector array.[10] Again, experimental details

can be found in Ref. 9.

Our extended level scheme, obtained by combining results from the two sets of experiments, is shown in Fig. 1.

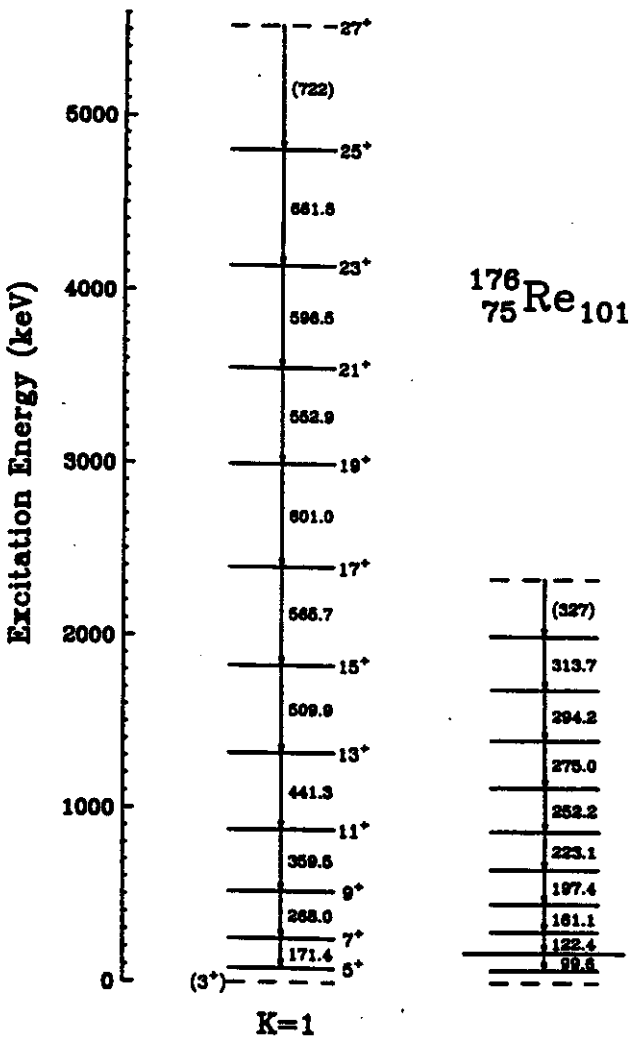

Fig. 1. Level scheme of ^{176}Re obtained using the ^{159}Tb(^{22}Ne,5nγ) and ^{165}Ho(^{16}O,5nγ) reactions, showing the two rotational bands populated most intensely. The position of these two bands with respect to the ground state and each other have not yet been completely worked out, so the relative excitation energies are normalized within each band. The dashed lines indicate the possibility of (unobserved) lower-lying states, and the longer line for the (second) state of the band displayed on the right indicates the possibility/probability that the band be based on this state.

The band shown at the left of Fig. 1 is the doubly-decoupled band. Such a band has spacings similar to the K=1/2 decoupled bands in the odd-proton nuclei nearby, and the band-head is not the state with J = K. This analog behavior is useful when assigning spins to members of the doubly-decoupled band. A survey of all the known doubly-decoupled bands in this region[11] and their relations with the corresponding odd-proton nuclei suggests that the lowest member of the band in ^{176}Re should have $J^{\pi} = 3^+$. The two-quasiparticle-plus-rotor calculations carried out by Santos et al. also favor this assignment. However, the lowest experimentally-observed state has $J^{\pi} = 5^+$. Both Santos et al. and we believe that the $5^+ \rightarrow 3^+$ transition was not observed because it is a highly-converted, low-energy E2 transition, the same reason that prevents the $9/2^- \rightarrow 5/2^-$ transitions from having been seen in some odd-mass Re nuclei.

The IBFFA predictions[8] for this doubly-decoupled, $\Delta J = 2$ band, which has the structure, $\pi h_{9/2}\,1/2^-[541] \times \nu\, p_{3/2}\,1/2^-[521]$, are shown in Fig. 2, where the 3^+ state is again suggested to be the band-head. We have some faith in this prediction because of the excellent agreement with experiment for the higher members of the band. The calculations predict the energy of the $5^+ \rightarrow 3^+$ transition to be 82.9 keV. Such an E2 transition could be picked up by an experiment having very good statistics and a low threshold (an experiment somewhat incompatible with those designed to extend the bands to higher spins). However, we should point out that the energy of the analogous unknown[12] transition in ^{175}Re has a strong influence on the IBFFA prediction for ^{176}Re.

It is worth mentioning the success of the IBFFA method in predicting other aspects of doubly-decoupling phenomena. The entire band is nominally the K = 1 triplet coupling, with the favored-signature (odd-spin) members depressed in energy with respect to the unfavored (even-spin) members. (Strictly speaking, K is not a

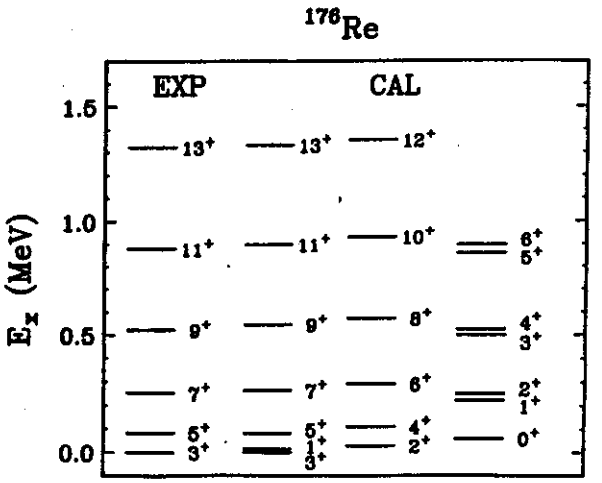

Fig. 2. Comparison of experimental data with IBFFA calculations for the doubly-decoupled band in ^{176}Re.

good quantum number in decoupled bands,[13,6] but it still serves as useful nomenclature.) The even-spin members are not--nor would they be expected to be--observed in our experiments. At the far right side of Fig. 2 is the prediction for the "K = 0" singlet coupling, also lying higher in energy and not observed.

Extending the doubly-decoupled band allows us to observe the band crossing. In Fig. 3 we plot the aligned angular momentum i_x vs angular frequency $\hbar\omega$ for this band in ^{176}Re, for decoupled bands in ^{177}Re and ^{175}W, and for ground-state bands in the cores, ^{176,174}W. Here $J_o = 38.2\ \hbar^2\text{MeV}^{-1}$ and $J_1 = 86.2\ \hbar^4\text{MeV}^{-3}$, derived from the first four data points used for ^{176}Re. The crossing frequencies and configurations for these bands are listed in Table I.

Table I.

Crossing Frequencies of the First Backbend in ^{176}Re and Other Related Bands.

Nucleus	Band	$\hbar\omega$(MeV)
^{176}Re	$\pi 1/2^-[541] \times \nu 1/2^-[521]$	0.29
^{174}W	ground-state	0.30
^{176}W	ground-state	0.30
^{175}W	$\nu 1/2^-[521]$	0.26
^{177}Os	$\nu 1/2^-[521]$	0.27
^{177}Re	$\pi 1/2^-[541]$	0.33

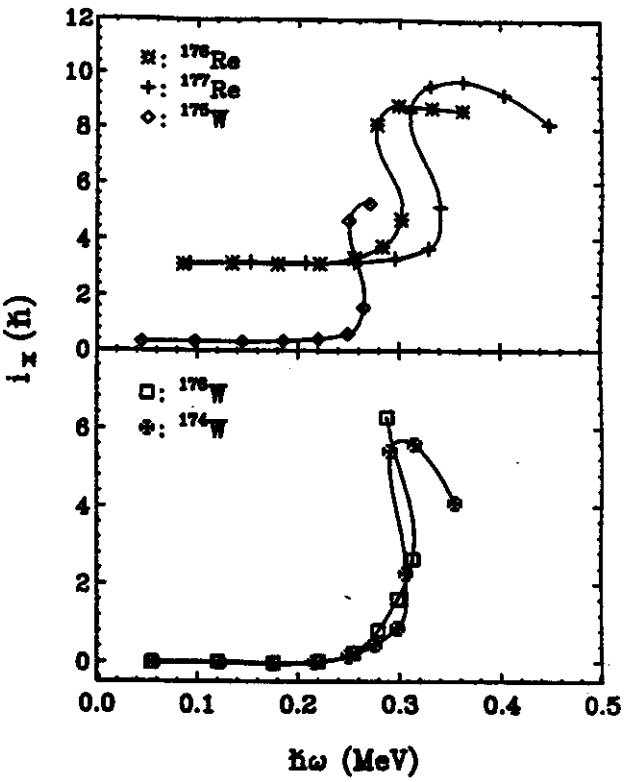

Fig. 3. Plot of aligned angular momentum i_x vs rotational frequency $\hbar\omega$ for the doubly-decoupled band in ^{176}Re and related bands in neighboring nuclei.

In this region of nuclei the $i_{13/2}$ neutrons are thought generally to be responsible for backbending. However, the $h_{9/2}$ protons are also believed to participate in the backbending process[14,15]--they could align at essentially the same frequency as the $i_{13/2}$ neutrons if they were not blocked, or the odd-proton state might drive the nucleus toward $\gamma = 0$ (or small positive values) and thereby delay backbending. For this doubly-decoupled band, backbending must be the result of aligning the $i_{13/2}$ neutrons because the $h_{9/2}$ proton orbitals are blocked. The effect of the odd-$h_{9/2}$ proton can be seen by comparing ^{177}Re (Ref. 16) with neighboring even-even nuclei.[17] A clear delay in reaching the crossing frequency in ^{177}Re can be seen. On the other hand, if the odd neutron is not in the $i_{13/2}$ state, then its effect will be to weaken the pairing correlation and make backbending occur earlier at a lower frequency. This can be seen in comparing ^{175}W (Ref. 18) and ^{177}Os (Ref. 19) with the even-even W nuclei. Now, the odd

proton in ^{176}Re should behave like the one in ^{177}Re; the odd neutron, like the one in ^{177}Os. To a first approximation, one would presume that the effects caused by the odd proton and neutron would simply be additive for odd-odd ^{176}Re. This appears to be so, with the result that the crossing-frequency shifts caused by the odd proton and odd neutron almost exactly cancel, so the crossing frequency is almost the same as for the even-even W nuclei. A similar situation was found for ^{172}Ta.[3]

We basically agree with Santos et al. for the energies of the transitions in the band shown on the right side of Fig. 1, but there is some uncertainty as to where the band starts, i.e., which state is the band-head. From our delay analysis and intensity ratios, the 99.6-keV transition appears to originate from a metastable state ($t_{1/2}$ = 21±7 ns). Santos et al. did not perform delay analysis. A second point is that they observed a 70.5-keV transition, which we could not see because of its being obscured by x rays. Thus, it is a moot point as to whether the first transition in this second band is 122.4 or 70.5 keV.

In addition to the indication from our delay analysis, a band having its first intraband transition at 123.8 keV and very similar spacings to this second band has recently been seen in ^{178}Re.[20] This band was assigned the configuration, $\pi 9/2^-[514] \times \nu_{13/2}$, a so-called compressed band,[6,13] resulting from strong coriolis coupling from the $i_{13/2}$ neutron state but little contribution from the proton state. There are two other bands in ^{178}Re that also have the neutron in an $i_{13/2}$ state. Comparing the crossing frequencies of these three bands in ^{178}Re with the analog bands in ^{177}Re (cf. Fig. 2 of Ref. 20), we find that the $\pi 9/2^-[514] \times \nu i_{13/2}$ band shows quite different behavior from the other two bands and is not nearly so compressed as the $\pi 5/2^+[402] \times \nu i_{13/2}$ band. Thus, we think the assignment might not be appropriate, i.e., the neutron might not be in an $i_{13/2}$ state.

Now, if the 122.4-keV transition is the one between the first two members of the band, the band resembles a regular rotational band, not overly compressed or staggered. Thus, its configuration should not involve states such as $1/2^-[541]$ or $7/2^+[633]$, which have large coriolis matrix elements. Here we would like to demonstrate how our IBFFA calculations can aid in narrowing down the possible configurations. In Fig. 4 we show the predictions[8,9] for eight rotational bands, the most likely couplings of observed odd-particle states from neighboring odd-mass nuclei. As expected, bands 5-8, those involving $\pi 1/2^-[541]$ or $\nu 7/2^+[633]$ states, are highly compressed and/or staggered, in disagreement with experimental data. None of the four remaining bands gives such excellent agreement that we can single it out as the correct configuration; however, bands $1(K^\pi = 2^-)$ and $4(7^+)$ give somewhat better spacings than the other two.

A straightforward method for emphasizing irregularities in band spacings is the so-called trumpet plot, a plot of $(E_J - E_{J-1})/2J$ vs $2J^2$. We show such a plot in Fig. 5 for both calculated and experimental energies, assuming four likely K values. The compression, especially between the first two members, shows clearly for the calculated 8^- band, as does the staggering, resulting from the $\pi 1/2^-[521]$ state for the 2^- band. Based on the comparisons shown in Fig. 5, the most likely configuration for this second band in ^{176}Re appears to be $K^\pi = 7^+, \pi 9/2^-[514] \times \nu 5/2^-[512]$. However, we emphasize that this comes as the result of a model-dependent argument--more experimental data, especially those involving the connection between this band and the ground state, will be needed to make the assignment definite.

In this report we have shown an extended level scheme for ^{176}Re, based on in-beam γ-ray

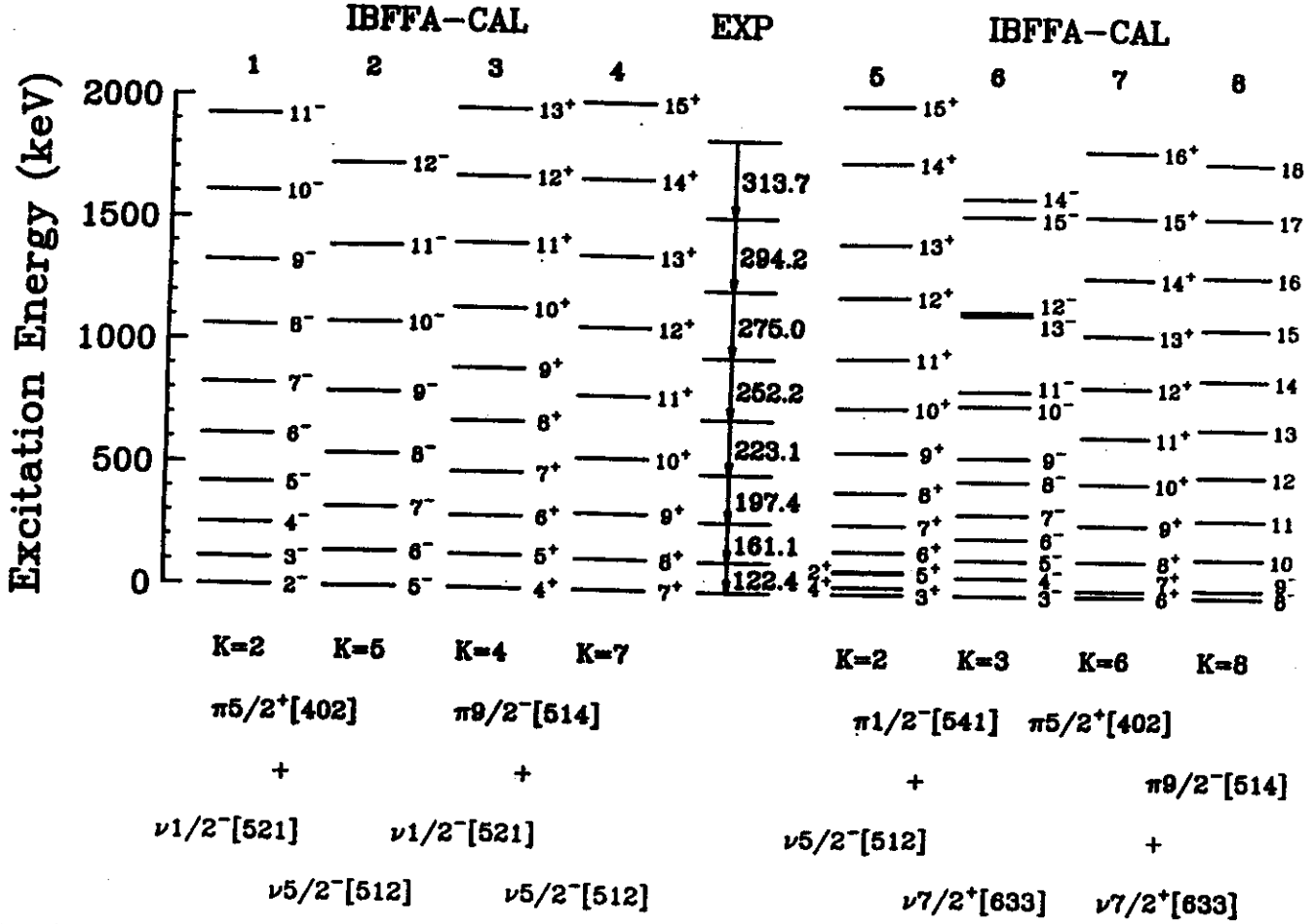

Fig. 4. IBFFA-calculated predictions for states in the eight most likely contenders for the configuration of the second band in ^{178}Re. The experimental band is shown in the middle for comparison.

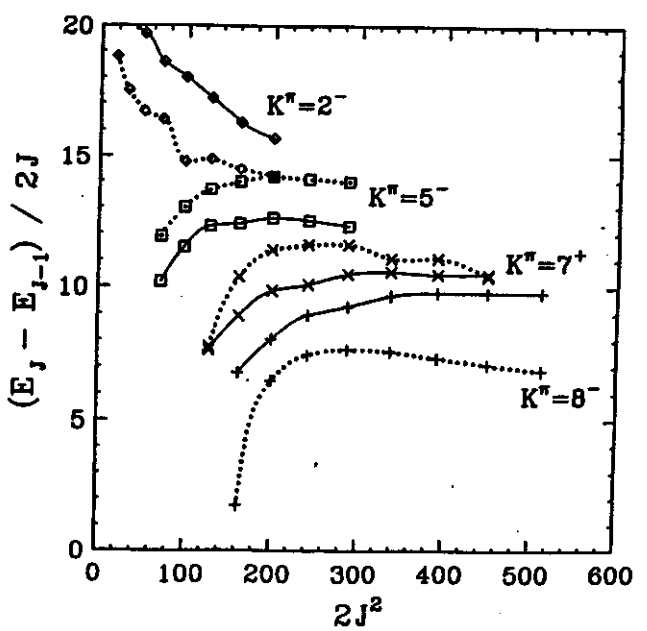

Fig. 5. IBFFA-calculated bands (connected by dotted lines) and experimental bands (solid lines) plotted in the manner of a trumpet plot to emphasize distortions in the level spacings. The experimental data were plotted in each case assuming the same value of K as the calculated band displayed with the same symbol.

studies following reactions induced by heavy-ion projectiles. Two main points emerge from this work: First, backbending has been observed for only the second time in a doubly-decoupled band. The crossing frequency is essentially the same as for the neighboring even-even cores. This comes about because the neutron and proton states have opposite driving effects, which cancel out almost exactly. This means that, although doubly-decoupled bands are indeed "decoupled," the decoupling is not so extreme as to preclude major effects by the odd particles on the behavior of the core. Second, IBFFA calculations, although certainly not a cure-all, can be a very useful aid in helping one decide among possible, likely odd-odd configurations.

---

a. Idaho National Engineering Laboratory EG &G, Idaho Falls, ID 83415.

References

1. M.F. Slaughter, R.A. Warner, T.L. Khoo, W.H. Kelly, and Wm.C. McHarris, Phys Rev. C 29(1984)114.
2. A.J. Kreiner, D.D. DiGregorio, A.J. Fendrik, J. Davidson, and M. Davidson, Phys. Rev. C 29(1984)1572.
3. A.J. Kreiner, D. Hojman, J. Davidson, M. Davidson, M. Debray, G. Falcone, C.W. Beausang, D.B. Fossan, R. Ma, E.S. Paul, S. Shi, and N. Xu, Phys. Lett. B 215(1988)629.
4. D. Santos, A.J. Kreiner, J. Davidson, M. Davidson, M. Debray, D. Hojman, and G. Falcone, Phys. Rev. C 39(1989)902.
5. Wm.C. McHarris, W.-T. Chou, J. Kupstas-Guido, and W.A. Olivier, in "Nuclei Off the Line of Stability", Ed. by R.A. Meyer and D.S. Brenner (American Chemical Society, Washington, DC, Symposium Series No. 324, (1986), Chap. 50.
6. A.J. Kreiner, J. Davidson, M. Davidson, D. Abriola, C. Pomar, and P. Thieberger, Phys. Rev. C 36(1987)2309; 37(1988)1338(E).
7. W.-T. Chou, Wm.C. McHarris, and O. Scholten, Phys. Rev. C 37(1988)2834.
8. W.-T. Chou, W.A. Olivier, Wm.C. McHarris, and O. Scholten, MSU NSCL Report MSUCL-713 (1990), submitted to Phys. Rev. C.
9. W.-T. Chou, Ph.D. Thesis, Michigan State University, 1989.
10. L. Hildingsson, C.W. Beausang, D.B. Fossan, W.F. Piel, A.P. Byrne, and G.D. Dracoulis, Nucl. Instr. Meth. A 252(1986)91.
11. W.A. Olivier, W.-T. Chou, R. Aryaeinejad, A. Rios, and Wm.C. McHarris, in "Exotic Nuclear Spectroscopy", Ed. by Wm.C. McHarris (Plenum Press, New York, 1990), Chap. 25.
12. J.R. Leigh, J.O. Newton, L.A. Ellis, M.C. Evans, and M.J. Emmott, Nucl. Phys. A 183(1972)177.
13. A.J. Kreiner, in "Exotic Nuclear Spectroscopy", Ed. by Wm.C. McHarris (Plenum Press, New York, 1990), Chap. 26.
14. J.D. Garrett, J. Nybery. C.H. Yu, J.M. Espino, and M.J. Godfrey, in "Proceedings of the International Conference on Contemporary Topics in Nuclear Structure Physics, Cocoyoc, Mexico, 1988", p. 699.
15. R. Bengtsson, ibid., p. 317.
16. C.X. Yang, J. Kownacki, J.D. Garrett, G.B. Hagemann, B. Herskind, J.C. Bacelar, J.R. Leslie, R. Chapman, J.C. Lisle, J.N. Mo, A. Simcock, J.C. Wilmott, W. Walus, L. Carlen, S. Johsson, J. Lyttkens, H. Ryde, P.O. Tjom, and P.M. Walker, Phys. Lett. B 133(1983)39.
17. G.D. Dracoulis, P.M. Walker, and A. Johnston, J. Phys. G. 4(1978)713.
18. P.M. Walker, G.K. Dracoulis, J. Johnson, J.R. Leigh, M.G. Slocombe, and I.F. Wright, J. Phys. G 4(1978)1655.
19. G.D. Dracoulis, C. Fahlander, and A.P. Byrne, Nucl. Phys. A 401(1983)490.
20. A.J. Kreiner, V.R. Vanin, F.A. Beck, Ch. Bourgeois, Th. Byrski, D. Curien, G. Duchene, B. Haas, J.C. Merdinger, M.G. Porquet, P. Romain, S. Rouabah, D. Santos, and J.P. Vivien, Phys. Rev. C 40(1989)R487.

ROTATIONAL BANDS AND POSSIBLE SUPERDEFORMATION IN ^{132}Pr

C.V. Hampton, A. Rios, R.M. Ronningen, W.A. Olivier, Wm.C. McHarris, F. McGowan[a], J. McNeill[a], N. Johnson[a], I. Yang Lee[a] and R. Aryaeinejad[b]

A fusion-evaporation experiment was conducted in November 1989, at the Holifield Heavy Ion Research Facility (HHIRF) at Oak Ridge National Laboratory. The objective of the study was to investigate the proton-neutron residual interaction in the odd-odd ^{132}Pr nucleus using γ-ray spectroscopy.

We selected the odd-odd Pr isotopes for our investigation primarily because they are located in the region where superdeformed rotational bands have been observed[1] and also because a moderate amount is known about the structure and systematics of the surrounding even-even and odd mass nuclei. Normal deformed nuclei have a nuclear axis ratio of $\beta \leq 0.3$. A superdeformed band refers to a larger deformation ($\beta \approx 0.5$) of the nucleus, resulting in a more elongated ellipsoidal shape. This was observed years ago with the discovery of "fission isomers" in the heaviest nuclei[2] and corresponds to a second minimum in deformation in the nuclear potential.[3] During the past few years discrete γ-rays from this second energy well were observed with the discovery of a superdeformed rotational band in ^{152}Dy.[4] Since then, superdeformed bands have been observed in three regions: 1) discrete bands in even-even nuclei near ^{152}Dy, 2) even-even and odd mass nuclei in the neutron deficient Ce region, 3) indications of bands via continuum γ-ray analysis in the odd-odd Re-Os region, and in odd-odd ^{150}Tb.

Band intensities for odd mass Tb are considerably greater than for nearby even-even nuclei. Blocking in the pairing force undoubtedly contributes to this, allowing the superdeformed band to exist at lower energies. If so, then blocking by both neutron and protron in odd-odd ^{152}Pr nucleus should make a superdeformed band even more readily observable.

We have performed fusion-evaporation CASCADE calculations to determine the most favorable reaction. Excitation functions showing the overlap of the cross sections of the 4n(^{132}Pr), 5n(^{133}Pr), α4n(^{129}La) and p4n(^{132}Ce) reaction channels is presented in Fig. 1. We chose the ^{100}Mo(^{37}Cl,5nγ)^{132}Pr reaction at 160 MeV.

The reaction was investigated using the Compton Suppression Spectrometer System at HHIRF.[5] The array consists of a 4π arrangement of 20 HPGe detectors, each surrounded by either NaI(Tl) or BGO compton suppression shields. There are 12 BGO (6 hexagonal, 6 pentagonal) and 9 NaI (4 hexagonal, 5 pentagonal) shields. In addition, a split annular BGO is located immediately behind each Ge crystal in order to catch the photons scattered in the forward direction. The BGO shields provide a compton background suppression factor of 5-6; the NaI shields provide a suppression factor two times lower. The energy resolution was determined to

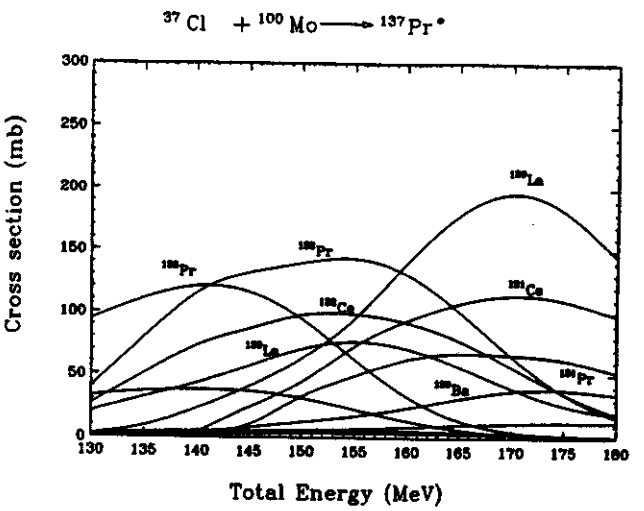

Fig. 1. Excitation function, calculated by CASCADE, predicting reaction cross sections for ^{100}Mo + ^{37}Cl reaction.

be 2.2 kev for the 1333 kev ^{60}Co transition (detector #3, θ=110.3).

The HHIRF Tandem electrostatic accelerator delivered a beam of ^{37}Cl (+7) at 160 Mev onto a ^{100}Mo target (thickness=0.5 mg/cm^2) which was obtained from LBL. Triple-coincidence γ-ray spectra and TAC information were acquired. A triple-coincidence γ-ray spectrum using detector #3, θ=110.3, is shown in Fig. 2. Peak centroids were obtained using the HHIRF gaussian fit routine, ASAP. Linear least squares analysis of spectra from ^{152}Eu, ^{133}Ba and ^{60}Co standards was used to obtain an isotropic energy calibration for each detector. The effects of Doppler shifts were cancelled by again calibrating each detector with the positions for known transitions in the reaction. Energy transitions were observed for $^{132}Pr^{*} \rightarrow {}^{132}Pr$, ^{132}Ce, ^{133}Pr and ^{133}Ce, corresponding to the 5n, p4n, 4n and p3n reactions, respectively.

Analysis of post experiment radioactive decay activities of the target indicate the presence of daughter nuclides from the above reactions plus the daughters from ^{129}La, as predicted by the CASCADE calculations.

Data analysis to determine more precise energies of transitions and structures is in progress. Angular distribution measurements should provide the multipolarity of the transitions. Lifetime measurements and moment of inertia calculations should establish the nuclear deformation ratio and the possible presence of superdeformation.

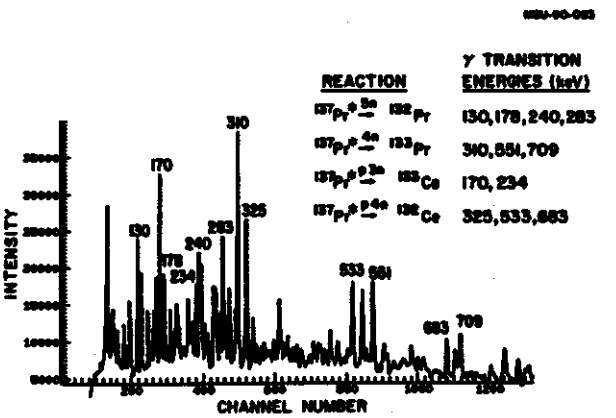

Fig. 2. Triple-coincidence γ-ray spectrum for the fusion-evaporation reaction from a ^{37}Cl beam at 160 MeV on a ^{100}Mo target, using the HHIRF Compton Suppression Spectrometer. (Ge #3, θ=110.3)

References

1. E.M. Beck et al., Phys. Rev. Lett. 58(1987)2182.
2. S.M. Polikanov et al., Zh. Eksp. Theor. Fiz. 42(1962)1464.
3. M.A. Deleplanque in "Exotic Nuclear Spectroscopy", ed. by Wm. C. McHarris (Plenum Press, New York, 1990), Chap. 21.
4. P.J. Twin et al., Phys. Rev. Lett. 57(1986)811.
5. Holifield Heavy Ion Research Facility, User's Handbook, Oak Ridge National Laboratory (1987)

a. Oak Ridge National Laboratory
b. EG & G